symmetry

MDPI

Article

Hamiltonian Model for Electron Heating by Electromagnetic Waves during Magnetic Reconnection with a Strong Guide Field

Fabio Sattin

Consorzio RFX (CNR, ENEA, INFN, Università di Padova, Acciaierie Venete SpA), 35127 Padova, Italy; fabio.sattin@igi.cnr.it

Abstract: Some recent published works have provided an exhaustive characterization of the plasma dynamics during magnetic reconnections in the presence of a magnetic guide field in MRX laboratory plasmas, including an assessment of the mechanisms that convert from magnetic energy to plasma kinetic energy. Among other results, the measurements indicate the existence of a correlation between the electron temperature and the generation of a spectrum of electric oscillations during the reconnection. In this work, we adapt to MRX conditions the well-known stochastic particle heating mechanism, frequently adopted in the astrophysical literature to justify ion heating by low-frequency large-amplitude electromagnetic waves. We show that, under MRX conditions. it may potentially provide a relevant contribution to electron energization.

Keywords: magnetic reconnection; electron heating; electron–wave interaction; Hamiltonian model; laboratory plasmas; MRX device; non-adiabatic dynamics

1. Introduction

Reconnections are ubiquitous processes in magnetized plasmas: laboratory, stellar, and planetary ones [1]. They involve sudden changes in the topology of the magnetic field, that rearranges into a state of lower energy. Part of the initial free energy is traveled away from the reconnection region by waves, or converted into the kinetic energy of ions and electrons. Reconnection is a complex process, which defies a unique description, since it is heavily dependent upon the geometry of the magnetic field and the physical conditions existing; it is, therefore, a topic still actively studied [2]. During reconnection, a lot of electromagnetic activity is produced in the form of quasi-steady fields, broadband turbulence, or coherent waves, which can interact with the ions and/or the electrons, delivering energy to the kinetic component of the plasma. A topic of current investigation concerns the mechanisms that allow energy to flow towards particles.

The Magnetic Reconnection eXperiment (MRX) is a device to study the fundamental physics issues of magnetic reconnection in a well-controlled laboratory environment [3]. We consider in this work the studies summarized in two recent papers by the MRX team [4,5], reporting a detailed campaign of measurements of plasma dynamics during reconnections in the presence of a guide magnetic field perpendicular to the reconnecting one. Measures were taken using a full 2D probe array for magnetic field reconstruction parallel to the (x, z) reconnection plane. Furthermore, an electrostatic probe, inserted near the reconnection region, allowed fast measurements of the electron density, temperature, and electric field. During reconnection, a quasi-steady electric field arises, parallel to the guide field, of amplitude $\langle E_y \rangle$ of order 100 V/m. Superimposed electric field oscillations in E_y appear. These oscillations appear as high-amplitude ($\delta E_y \simeq \langle E_y \rangle$), almost monochromatic (frequency $\nu \approx 2$ MHz, in the lower-hybrid wave frequency range) waves traveling along the electron outflow with a wavelength of the order of the thermal electron Larmor radius ($k\rho_e \approx 1$). The electron density fluctuations appear correlated with the electric field ones. Importantly, for this work, an increasing trend in the average electron temperature (of

Citation: Sattin, F. Hamiltonian Model for Electron Heating by Electromagnetic Waves during Magnetic Reconnection with a Strong Guide Field. *Symmetry* **2024**, *16*, 1095. https://doi.org/10.3390/sym16091095

Academic Editors: Fabio Reale and Paolo Pagano

Received: 18 July 2024
Revised: 12 August 2024
Accepted: 20 August 2024
Published: 23 August 2024

the order of 10 eV) near the X line with δE_y is observed. We refer to Figure 4 of paper [4], and in particular, to the red dots, corresponding to the high-guide-field case, where almost a doubling of T_e is observed in going from the smallest ($\approx$50 V/m) to the largest ($\approx$150 V/m) values of δE_y.

The second part of the study [5] is devoted to a characterization of the energy budget to identify the different ways through which magnetic energy is converted into particle energy. As far as the electron component is concerned, the study concludes that a relevant fraction of the energy is delivered to the electrons through parallel acceleration by the electric field $\langle E_y \rangle$ near the X-point or the reconnecting field, along the y-direction.

Given the high level of electric fluctuations with respect to the steady component, and the correlation between them and the electron temperature, found in [4], it appears reasonable to investigate how and to what extent the oscillatory part may contribute to the electron energization. This is the purpose of this work. We propose that a fraction of the electron heating may occur via interaction with low-frequency high-amplitude electromagnetic waves. This mechanism has frequently been invoked in the astrophysical literature, often as a candidate for ion heating by Alfvèn waves, but its range of application is more widespread [6–19]. In the present case, we do not refer specifically to a coherent mode: by the term "wave", we mean a traveling electromagnetic plane wave Fourier component out of a whole spectrum. Since the frequency range of the experimental spectrum is fairly narrow, retaining just one frequency component within the model appears to be a reasonable simplification. We sketch a rough Hamiltonian model of wave–particle interaction in the presence of a strong guide magnetic field, in a simplified geometry, representative of MRX conditions. We show that, when feeding the model with MRX plasma parameters, we are able to recover quantitatively the measured amount of heating, in terms of temperature gain per electron. We justify our test-particle approach based on the fact that MRX plasmas are relatively low-β, $\beta \approx 0.5$.

Finally, as a spin-off, we discuss wave–particle correlations along the parallel direction, reminiscent of the collisionless Landau damping mechanism, which arise spontaneously within our framework.

2. Methods

Throughout this study, we will restrict ourselves close to the X line, where the reconnecting component of the magnetic field is small and will be neglected in comparison to the perpendicular guide field $\mathbf{B}_g$.

Within the Hamiltonian formulation, any electric and magnetic field is described in terms of potentials. The guide magnetic field is

$$\mathbf{B}_g = \nabla \times \mathbf{A}_g, \quad \mathbf{A}_g = -B_0 x\, \hat{z} \tag{1}$$

To this field, we add a monochromatic electromagnetic wave:

$$\mathbf{A}_w = \frac{b}{k} \cos(kx - \omega t)\, \hat{y} \tag{2}$$

The wave has both magnetic and electric components:

$$\mathbf{B}_w^{(m)} = b \sin(kx - \omega t)\, \hat{z}, \quad \mathbf{E}_w^{(m)} = -\frac{b\omega}{k} \sin(kx - \omega t)\, \hat{y} \tag{3}$$

Notice that the oscillating electric field is oriented along the direction out of the reconnection plane and parallel to the guide field, like in the experiment. We provide in Figure 1 a sketch of the experimental arrangement: we show a section of the reconnecting field in the (x, z) plane; the arrow along the y-axis represents the direction of the guide field, while the sinusoidal curve stands for the wave propagating along the x-axis.

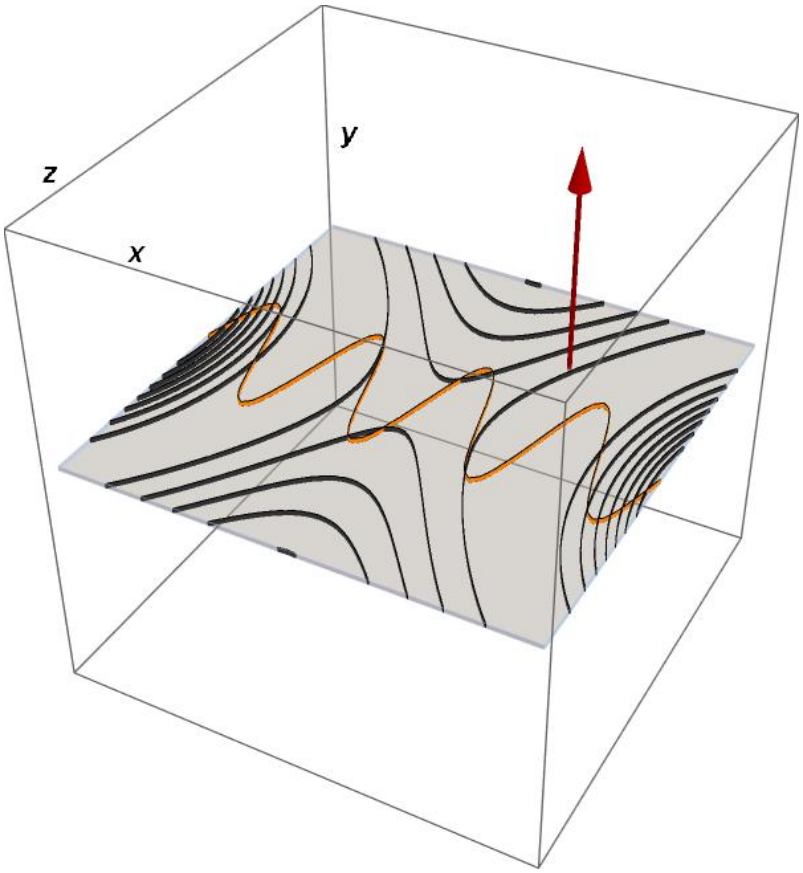

Figure 1. A rough sketch of the experimental arrangement. The field lines of the reconnecting magnetic fields are shown in a 2D section onto the (x, z) plane. The red arrow marks the direction of the guide field. The orange curve stands for the wave propagating along the x-axis.

In MRX, fluctuations superimpose upon a mean flow, driven by an average electric field and braked by collisions [4]. Here, we place ourselves in a reference frame moving with the mean flow, thus treating electrons as initially at rest along the y-axis, and neglecting both collisions and the stationary electric field.

In the following lines, for convenience, we will be using dimensionless quantities: time is given in units of Ω^{-1}, with $\Omega = qB_0/m$ the Larmor angular frequency. Lengths are normalized to the thermal Larmor radius $\rho = \sqrt{qT_e/m}$, where T_e is the measured electron plasma temperature and q, m are the electron charge and mass. The single-particle Hamiltonian is written,

$$\begin{aligned} H &= \frac{p_x^2}{2} + \frac{1}{2}\left(p_y - A_w\right)^2 + \frac{1}{2}\left(p_z - A_g\right)^2 \\ &\equiv \frac{p_x^2}{2} + \frac{x^2}{2} + \frac{b^2}{4k^2}\cos(2kx - 2\omega t) \end{aligned} \tag{4}$$

Since H does not depend upon the coordinates y, z, the momenta p_y, p_z are constant of the motion. They can be dropped from the Hamiltonian using a gauge transform of $\mathbf{A}$. A constant term $(b/2k)^2$, which represents just an offset, has been dropped alike. The Hamiltonian (4), but for the inessential factor $2k$ in the argument of the trigonometric term, is in the paradigmatic form

$$H' = \frac{p_x^2}{2} + \frac{x^2}{2} + a\cos(x - \omega t) \tag{5}$$

Note that H and H' depend just upon the single x spatial coordinate. Had we accounted for the reconnecting component of the magnetic field, the system would have been

fully three-dimensional. The Hamiltonian (5) has been extensively studied in the cited literature [6–19]. Since the Hamiltonian features a time dependence ωt that is slow compared to the cyclotron motion (in our dimensionless units, $\omega \simeq 10^{-3}$), one might naively conjecture that the corresponding dynamics are always adiabatic and reversible, i.e., if the wave is turned on for some time, and then switched off, the initial and final particle energy are the same. The literature cited above shows, instead, that this is true only for small wave amplitudes; there is a transition from adiabatic to non-adiabatic dynamics in correspondence of a trespassing the threshold $a = 1$. This condition corresponds to the appearance of a slow (moving with the wave frequency) separatrix in the particle phase space. In the static case ($\omega = 0$), the separatrix divides orbits into totally disjointed basins while, in the dynamical regime, it is permeable. Close to the separatrix, the period of the orbit becomes very large, exceeding the wave period. Thus, the adiabaticity hypothesis, which relies upon the particle orbit period being much smaller than the wave period, breaks down; any crossing of the separatrix is an essentially irreversible process. Since the separatrix is an iso-energy curve in the phase space, each crossing corresponds to moving between disjointed basins at different energies: the initial and final particle energies are different. Therefore, a net energy transfer between particle and wave may effectively take place. (The threshold condition $a = 1$ places a constraint upon the wave amplitude which is often difficult to satisfy in laboratory (and sometimes also astrophysical) plasmas, where fluctuations are ordinarily small with respect to the mean fields. Although it is not relevant to the present work, we mention that recently, we showed that this threshold is not always needed, since under some conditions it can be traded for a threshold upon the duration of the wave–particle interaction, in a way reminiscent of quantum-mechanics indeterminacy relations: see the paper [20]). This result is made visual in Figure 2: each of the 16 subplots is a snapshot of the instantaneous state of the system in the plane (kx, p_x) taken at consecutive time intervals $\Delta t = \pi/(8\omega)$, from left to right and from top to bottom. The colored contour levels label the instantaneous iso-energy curves $p_x^2/2 + x^2/2 + A\cos(kx - \omega t) = \text{constant}$. The red dots mark the position of 30 particles initialized close to each other near the origin $(x = 0, p_x = 0)$ (left-top subplot). While time evolves, the particles spread along almost iso-energy curves but, ultimately, a fraction of them crosses the newborn separatrix (third row) and remains energetically separated from the others.

We enclose in the Supplementary Materials a video clip illustrating dynamically the same behavior: the motion of two initially close particles (red and green dots) is tracked in the (x, p_x) plane, superimposed on the instantaneous iso-energy levels, which progressively become detached in correspondence of each jump across the separatrix and the X-point. The energy of the two particles differs as well.

The threshold amplitude is written as $a_{thre} = b^2 = 1$. The amplitude of the electric field associated to the wave is $|E_w| = \omega b/k$; hence, the threshold condition can be written as $|E_w| \geq \omega/k$. In physical units, it becomes

$$|E_w| \geq (\omega\,\rho)\,B_0\,(k\,\rho)^{-1} = \frac{\omega}{\Omega} u_{th}\,B_0\,(k\,\rho)^{-1} \tag{6}$$

where u_{th} is the thermal speed and Ω is the electron Larmor frequency. The average energy gained per particle in the non-adiabatic regime is a question that, quantitatively, has not yet received a full investigation. Some partial investigations are reported in [15], but only cold particles were considered there, i.e., their initial distribution was practically mono-energetic and close to zero. In this paper, we are going to repeat the exercise using a realistic thermal initial distribution.

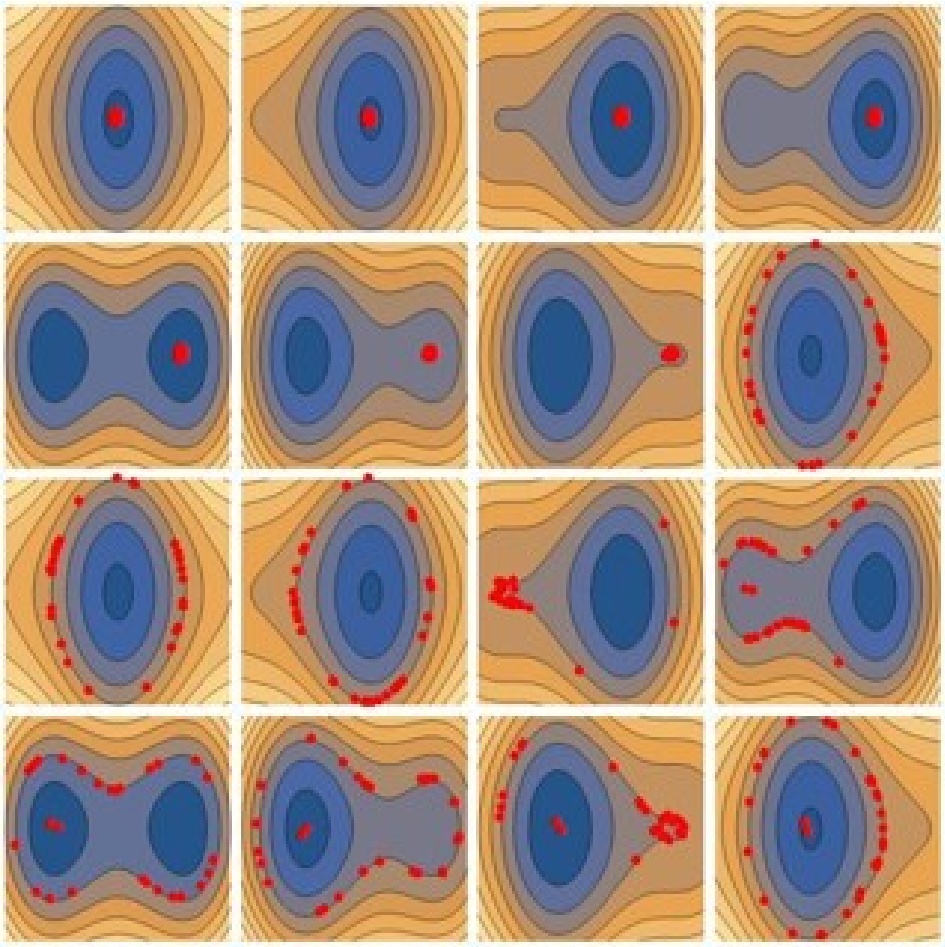

Figure 2. Snaphots at consecutive time intervals $\Delta t = \pi/(8\,\omega)$ of the state of the particle: from left to right and from top to bottom. The colored contour levels label the instantaneous iso-energy curves $p_x^2/2 + x^2/2 + A\cos(kx - \omega t) = \text{constant}$. The red dots mark the corresponding instantaneous position of 30 particles. The particles are initialized close to each other near the origin $(x = 0, p_x = 0)$ (left-top subplot). At the end of the simulation (corresponding to two full wave periods), part of the particles is left with an energy close to their initial value, while another fraction lies now on a different energy curve. The figure is reused from the original publication [15].

Hamilton equations from Equation (4) were integrated in time using one symplectic algorithm built into Wolfram's Mathematica 12.0 software ("NDSolve" routine, choosing the "SymplecticPartitionedRungeKutta" method of fourth order), and another one implemented from ref. [21]. Here below, we provide the results of a scan performed varying the wave amplitude $A = (b/(2k))^2$. The numerical strategy is the same employed elsewhere: we switch on and off the wave through a shape function $f(t) : A \to A\,f(t)$, with

$$f(t) = \frac{1}{4}\left(1 + \tanh\left(\frac{t - t_S}{\Delta t}\right)\right)\left(1 + \tanh\left(\frac{t_F - t}{\Delta t}\right)\right) \tag{7}$$

In this expression, t_S, t_F represent the start and end time of the perturbation, and Δt is the time scale for switch-on and -off. By comparing the particle energy before and after the switching of the wave, we obtain the amount of heating. For each value of A, 2400 independent trajectories were evolved. The initial conditions were randomly sampled from a thermal distribution, i.e., E_0 and r picked up, respectively, from a zero-mean, unit-variance normal distribution, and from the uniform distribution in $(0, 1)$, and $x(0) = (rE_0)^{1/2}$, $p(0) = ((1-r)E_0)^{1/2}$. All parameters were taken from MRX measurements. Using non-normalized quantities: $B_0 = 110$ Gauss, $T_e = 8$ eV, $k\rho = 1$, $\omega/(2\pi) = 2$ MHz. The shape function $f(t)$ grows up and

falls down over the MRX time scale for the bursts of electromagnetic activity: $t_S = 2.5\,\mu s$, $t_F = 7.5\,\mu s$, $\Delta t = 1\,\mu s$; this yields an effective duration time of the electron–wave interaction of roughly 5 μs, which, based upon the figures in [4] (see their Figure 2), appears reasonable. The temperature, for each value of the electric field, was computed as the average energy of the particles after the interaction with the wave had been switched off.

3. Results

The main result of this work is summarized in Figure 3. The threshold amplitude of Equation (6) corresponds to 85 V/m for the parameters employed. There is energy gain by the electrons only beyond this threshold: compare the two leftmost points with the others. The figure should be compared with Figure 4 of the paper [4], in particular, with the red dots that correspond to the case with the largest guide field, closest to the geometry employed in the present work; there, the electron temperature rises from slightly more than 7 eV to about 10 eV over the range 50–150 V/m, nicely consistent with our result.

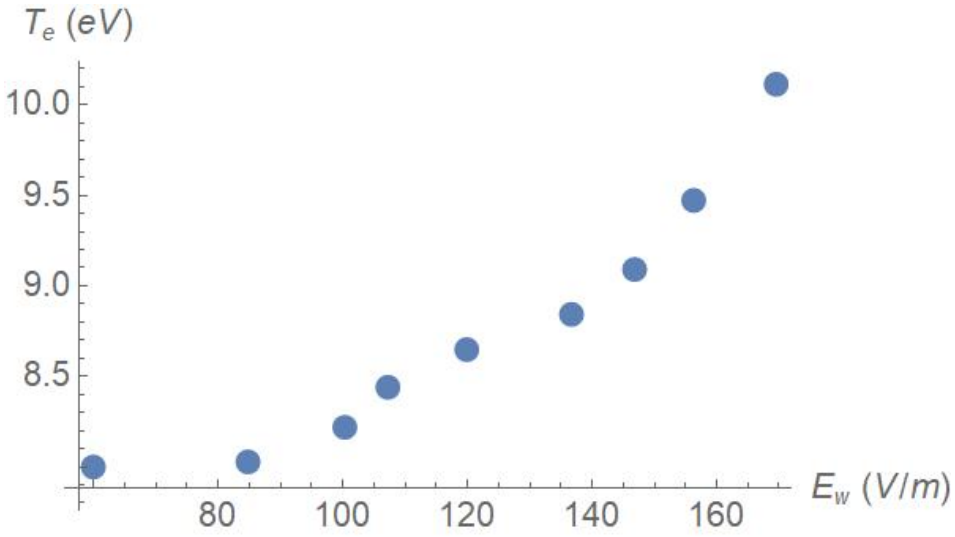

Figure 3. Final temperature (average energy of the test particle) when the initial temperature $T_e = 8$ eV versus the amplitude of the wave electric field. The threshold value (Equation (6)) is $E_w = 85$ V/m, corresponding to the second point from the left.

Indeed, it is possible to advance a conjecture: according to the paper [4], electric fluctuations superimpose to a background quasi-static electric field parallel to the guide magnetic field, whose typical value is about 80 V/m. The electron collision time for a 10 eV, 10^{13} cm^{-3} plasma is $\tau_{coll} \approx 10^{-7}$ s. Over this time scale, the energy gained by an electron due to parallel acceleration is $\Delta K \approx O(10)$ eV. Thus, we may envisage the following scenario: the baseline electron temperature, $\approx 6 \div 8$ eV, is due to electron energization by parallel electric fields. This conclusion is consistent with the analysis carried out in [5]. Waves add a further contribution that, depending upon their amplitude, may amount up to $2 \div 3$ eV.

In order to give an insight about the typical dynamics experienced by the electrons during their interaction with the wave, we plot in Figure 4 a sample of the time trace of the electron's kinetic energy, $p_x(t)^2/2$, alongside the corresponding time trace of the wave as experienced by the particle: $f(t)\cos(kx(t) - \omega t)$. In particular, we pay attention to the wild energy fluctuations during the time interval t = 5000–15,000, when $f \approx 1$. They greatly exceed the final stationary energy of the particle, but only transiently; in the sub-threshold case, ultimately, the electron lands back to its initial energy once the wave has disappeared.

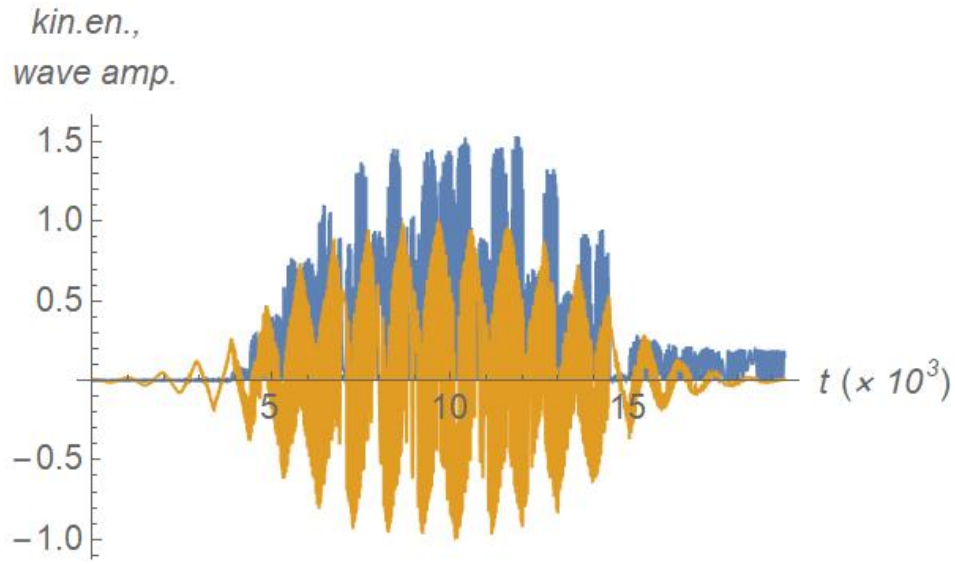

Figure 4. An example of time trace of one simulation. The blue curve is the kinetic energy $p_x^2(t)/2$, the yellow curve is $f(t)cos(kx(t) - \omega t)$. This run features $E_w = 170$ V/m—twice the threshold for the onset of nonadiabatic motion, and an initially almost static particle: $x(0) = 0, p_x(0) = 0.075$.

In Figure 5, we show the probability distribution of the initial and final particle momenta p_x for the case with $E_w = 170$ V/m. Each distribution has been computed by taking the initial (respectively, final) value of the momentum for all the 2400 independent trajectories. Interestingly, the final distribution remains fairly close to a thermal (normal) curve. This result was not obtained from earlier studies using monoenergetic initial distributions, and is comforting since experimental measurements hint at a true heating, not just electron energization.

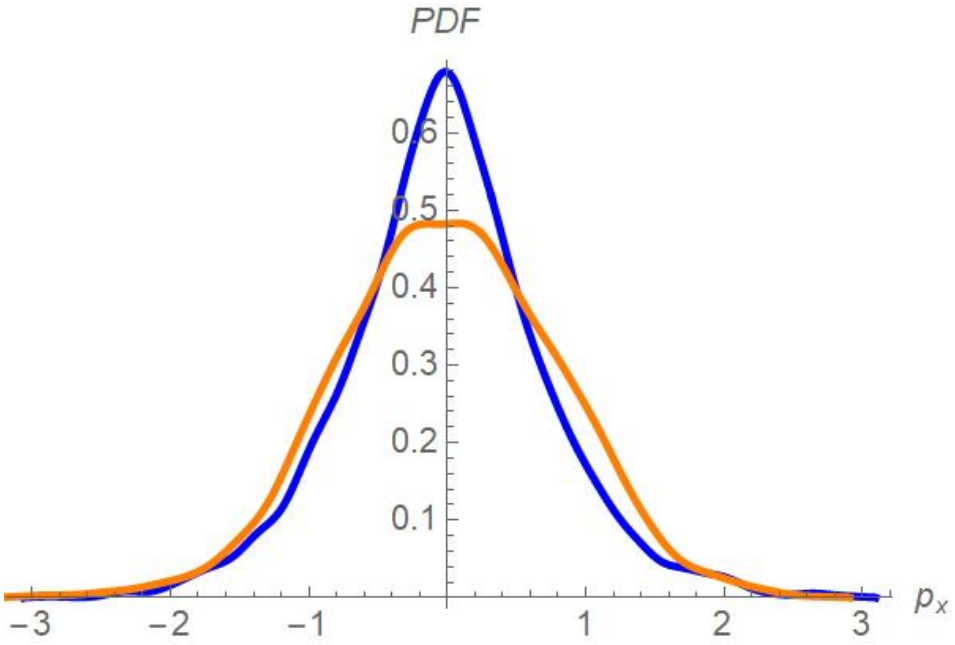

Figure 5. Probability distribution of the initial (blue) and final (orange) momentum distribution for the case with $E_w = 170$ V/m, computed over 2400 independent trajectories.

We remark, even though the wave electric field is parallel to the guide magnetic field, energization of the electrons occurs along the x-direction, perpendicular to **B**. Since Hamilton's equation for the motion along the magnetic field is written as $dz/dt = -A_w(x,t)$

(setting $p_z = 0$), when the wave vanishes ($A_w \to 0$), we are sure that the particle stops moving along z; no energy is acquired along the parallel direction.

We conclude with a spin-off of the above analysis. Our simulations do not involve interactions between particles, and in particular, between ions and electrons; therefore, the subject of the anomalous resistivity is outside the scope of this work. Yet, the analysis of the particle dynamics reveals interesting aspects. In Figure 6, we plot one time trace of the quantity $\sin(kx - \omega t)$, where $x = x(t)$ is the computed trajectory. The plot refers to the flat-top phase, where $f(t) \approx 1$. Although the plot refers to just one case, the inspection of several trajectories shows that the picture is generic: the particle trajectory exhibits a quasi-periodic trend, with intervals where it slowly drifts around two attractors, placed at the phase $= \pm 90°$, interrupted by sudden jumps from the one to the other.

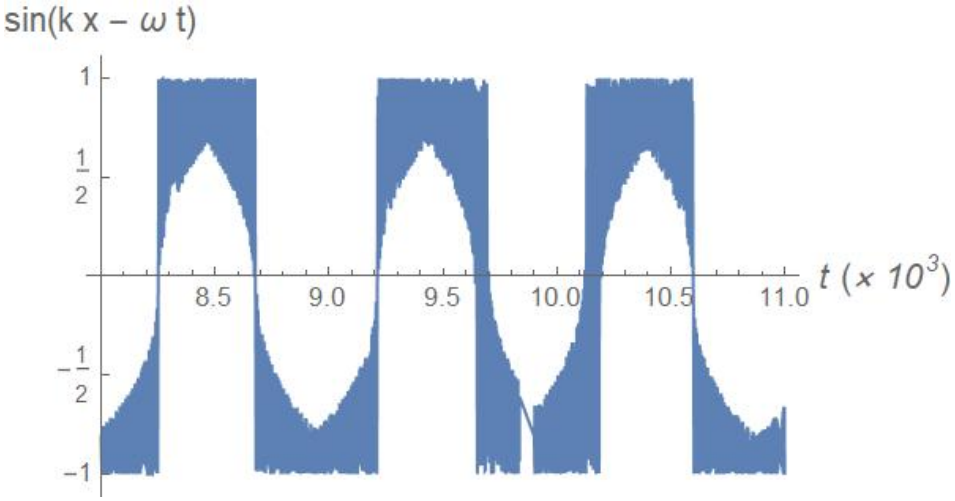

Figure 6. Time trace of $\sin(k\,x - \omega\,t)$ for one trajectory. Here, $E_w = 130$ V/m, $x(0) = 0.2$, $p_x(0) = 0.075$.

From Equation (4), we retrieve the equation of motion along y:

$$\frac{dy}{dt} = -\frac{b}{k}\cos(kx - \omega t) \tag{8}$$

where we have set $p_y = 0$, consistent with our choice of the initial conditions. After another derivative, we obtain Newton's law

$$\frac{d^2y}{dt^2} = -\omega\frac{b}{k}\sin(kx - \omega t) \tag{9}$$

The dynamics of Figure 6 consists of finite intervals where the particle stays almost in phase with the peaks of the electric field: ($|\sin(kx - \omega t)| \approx 1$), which is a feature of the Landau damping. This condition, which corresponds to the state of maximal acceleration by the electric field, is unstable since it is incompatible over long periods with the $dy/dt \approx 0$ condition from Equation (8); thus, the system jumps repeatedly between the two fixed points. Yoo et al. [4] introduce the anomalous drag term $D = -\langle \delta n_e \delta E \rangle / \langle n_e \rangle$, which quantifies the correlation between the particle and the electric field oscillations and the contribution to the resistivity by the fluctuating terms. Within our framework, the analog of D, normalized to the electric field amplitude, is

$$D' = \langle \delta(x - x(t)) \sin(kx(t) - \omega t) \rangle \tag{10}$$

where $x(t)$ is the particle trajectory, and the average $\langle \ldots \rangle$ is performed both over time and over all the trajectories.

In our case, there is no symmetry-breaking term; correlated and anti-correlated phases are equally likely, thus D' vanishes. However, we may speculate about what would

happen if an efficient symmetry-breaking mechanism, that allows only correlated (or anti-correlated) phases to survive, were added. If we average $\sin(kx(t) - \omega t)$ over just the time windows where it is positive, we obtain $\langle \sin(kx(t) - \omega t) \rangle_{>0} \approx 0.84 = \cos(32^\circ)$, which compares fairly well with the $\cos(30^\circ)$ figure coming from the measurements of Yoo et al. By comparison, a perfectly sinusoidal trend would yield $\int_0^\pi dx \, \sin(x)/\pi = \cos(50^\circ)$. All this is highly speculative, yet it is suggestive that the observed correlation might arise as a consequence of this kind of resonance.

4. Conclusions

In this work, we have presented a proposal for electron energization by low-frequency high-amplitude electromagnetic waves produced during magnetic reconnection. The physical mechanism is well established in the literature. It is based upon the appearance of a moving separatrix in the particle phase space whose crossing breaks the adiabaticity of the motion and allows for an irreversible transfer of energy between wave and particle. The model is not self-consistent, since the wave spectrum is given from the outset and no backreaction of the particle component onto the magnetic field is accounted for. Within a first-order approximation, this is justified on the basis that MRX plasmas are relatively low-beta. When applied to the MRX published data, the model has foreseen a level of energization close to that measured, suggesting that it could be a relevant player in the overall energy budget, comparable to the energization due to parallel acceleration along steady electric fields. Indeed, a reasonable guess is that the static parallel electric field heats the electron up to the $6 \div 8$ eV baseline value, while the wave contribution justifies the remaining $2 \div 3$ eV that appear in Figure 4 of the paper [4].

Supplementary Materials: The following supporting information can be downloaded at: https://www.mdpi.com/article/10.3390/sym16091095/s1, Video S1: video.

Funding: This research received no external funding.

Data Availability Statement: The source code and the datasets are available from the author upon request.

Acknowledgments: Discussions with D. Bonfiglio, S. Cappello, D.F. Escande, and M. Gobbin are gratefully acknowledged. The author wishes to thank the anonymous referees for their valuable suggestions.

Conflicts of Interest: The author declares no conflicts of interest.

References

1. Yamada, M.; Kulsrud, R.; Ji, H. Magnetic reconnection. *Rev. Mod. Phys.* **2010**, *82*, 603–664. [CrossRef]
2. Ji, H.; Daughton, W.; Jara-Almonte, J.; Stanier, A.; Yoo, J. Magnetic reconnection in the era of exascale computing and multiscale experiments. *Nat. Rev. Phys.* **2022**, *4*, 263–282. [CrossRef]
3. Yamada, M.; Ji, H.; Hsu, S.; Carter, T.; Kulsrud, R.; Bretz, N.; Jobes, F.; Ono, Y.; Perkins, F. Study of driven magnetic reconnection in a laboratory plasma. *Phys. Plasmas* **1997**, *4*, 1936–1944. [CrossRef]
4. Yoo, J.; Ng, J.; Ji, H.; Bose, S.; Goodman, A.; Alt, A.; Chen, L.; Shi, P.; Yamada, M. Anomalous resistivity and electron heating by lower hybrid drift waves during magnetic reconnection with a guide field. *Phys. Rev. Lett.* **2024**, *132*, 145101. [CrossRef]
5. Bose, S.; Fox, W.; Ji, H.; Yoo, J.; Goodman, A.; Alt, A.; Yamada, M. Conversion of magnetic energy to plasma kinetic energy during guide field magnetic reconnection in the laboratory. *Phys. Rev. Lett.* **2024**, *132*, 205102. [CrossRef]
6. Karney, C.F.F. Stochastic ion heating by a lower hybrid wave: II. *Phys. Fluids* **1979**, *22*, 2188–2209. [CrossRef]
7. Drake, J.F.; Lee, T.T. Irreversibility and transport in the lower hybrid drift instability. *Phys. Fluids* **1981**, *24*, 1115–1125. [CrossRef]
8. McChesney, J.M.; Stern, R.A.; Bellan, P.M. Observation of fast stochastic ion heating by drift waves. *Phys. Rev. Lett.* **1987**, *59*, 1436–1439. [CrossRef]
9. Chen, L.; Lin, Z.; White, R. On resonant heating below the cyclotron frequency. *Phys. Plasmas* **2001**, *8*, 4713–4716. [CrossRef]
10. Kolesnychenko, O.Y.; Lutsenko, V.V.; White, R.B. Ion acceleration in plasmas with Alfvén waves. *Phys. Plasmas* **2005**, *12*, 102101. [CrossRef]
11. Wang, C.B.; Wu, C.; Yoon, P.H. Heating of ions by Alfvén waves via nonresonant interactions. *Phys. Rev. Lett.* **2006**, *96*,125001. [CrossRef] [PubMed]
12. Li, X.; Lu, Q.; Li, B. Ion pickup by finite amplitude parallel propagating Alfvén waves. *Astrophys. J.* **2007**, *661*, L105. [CrossRef]
13. Guo, Z.; Crabtree, C.; Chen, L. Theory of charged particle heating by low-frequency Alfvén waves. *Phys. Plasmas* **2008**, *15*, 032311. [CrossRef]

14. Chandran, B.D.G.; Li, B.; Rogers, B.N.; Quataert, E.; Germaschewski, K. Perpendicular ion heating by low-frequency Alfvén-wave turbulence in the solar wind. *Astrophys. J.* **2010**, *720*, 503. [CrossRef]
15. Escande, D.F.; Gondret, V.; Sattin, F. Relevant heating of the quiet solar corona by Alfvén waves: A result of adiabaticity breakdown. *Sci. Rep.* **2019**, *9*, 14274. [CrossRef] [PubMed]
16. Stasiewicz, K. Stochastic ion and electron heating on drift instabilities at the bow shock. *MNRAS* **2020**, *496*, L133. [CrossRef]
17. Stasiewicz, K.; Eliasson, B. Stochastic and quasi-adiabatic electron heating in quasi-parallel shocks. *Astrophys. J.* **2020**, *904*, 173. [CrossRef]
18. Yoon, Y.D.; Bellan, P.M. How Hall electric fields intrinsically chaotize and heat ions during collisionless magnetic reconnection. *Phys. Plasmas* **2021**, *28*, 022113. [CrossRef]
19. Cerri, S.S.; Arzamasskiy, L.; Kunz, M.W. On stochastic heating and its phase-space signatures in low-beta kinetic turbulence. *Astrophys. J.* **2021**, *916*, 120. [CrossRef]
20. Sattin, F.; Escande, D.F. Thresholdless stochastic particle heating by a single wave. *Phys. Rev. E* **2023**, *107*, 065201. [CrossRef]
21. McLachlan, R.I.; Atela, P. The accuracy of symplectic integrators. *Nonlinearity* **1992**, *5*, 541. [CrossRef]